

# Nano Based Sensor for Assessment of Weaponry Structural Degradation

Christina L. Brantley<sup>1</sup>, Eugene Edwards,<sup>1</sup> Paul B. Ruffin<sup>2</sup>, Michael Kranz<sup>3</sup>  
U. S. Army Research, Development, and Engineering Command<sup>1</sup>  
Redstone Arsenal, Alabama 35898

Alabama A&M University<sup>2</sup>  
College of Physics, Chemistry, and Engineering  
Normal, Alabama 35811

EngeniusMicro, LLC<sup>3</sup>  
228 Holmes Ave NE  
Huntsville, AL 35801

## ABSTRACT

Missiles and weaponry-based systems are composed of metal structures that can degrade after prolonged exposure to environmental elements. A particular concern is accumulation of corrosion that generally results from prolonged environmental exposure. Corrosion, defined as the unintended destruction or deterioration of a material due to its interaction with the environment, can negatively affect both equipment and infrastructure. System readiness and safety can be reduced if corrosion is not detected, prevented and managed. The current corrosion recognition methods (Visual, Radiography, Ultrasonics, Eddy Current, and Thermography) are expensive and potentially unreliable. Visual perception is the most commonly used method for determining corrosion in metal. Utilization of an inductance-based sensor system is being proposed as part of the authors' research. Results from this research will provide a more efficient, economical, and non-destructive sensing approach. Preliminary results demonstrate a highly linear degradation within a corrosive environment due to the increased surface area available on the sensor coupon. The inductance of the devices, which represents a volume property of the coupon, demonstrated sensitivity to corrosion levels. The proposed approach allows a direct mass-loss measurement based on the change in the inductance of the coupon when placed in an alternating magnetic field. Prototype devices have demonstrated highly predictable corrosion rates that are easily measured using low-power small electronic circuits and energy harvesting methods to interrogate the sensor. Preliminary testing demonstrates that the device concept is acceptable and future opportunities for use in low power embedded applications are achievable. Key results in this paper include the assessment of typical Army corrosion cost, degradation patterns of varying metal materials, and application of wireless sensors elements.

*This information product is approved for public release. The views and opinions of its authors do not necessarily state or reflect those of the U.S. Government or any agency thereof. Reference to any specific commercial product, process, or service by trade name, trademark, manufacturer, or otherwise does not necessarily constitute or imply its endorsement, recommendation, or favoring by the U.S. Government or any agency thereof."*

# 1. INTRODUCTION

The Department of Defense (DoD) is actively pursuing improved corrosion prevention and monitoring approaches to reduce maintenance costs and improve operational readiness. In 2006, corrosion-related costs of DoD equipment maintenance totaled \$19.4 billion, or 24 percent of the total cost of maintenance. In addition to cost, 16% of equipment downtime was attributed to corrosion in 2009. Variability in corrosion itself is a particular challenge for monitoring because the predictions for initiation location are inaccurate, so monitoring solutions are applied to general problem areas. The size-scale of typical sensors results in point location monitoring, and identical sensors under seemingly identical conditions show drastically different responses. Sensors with increased repeatability and confidence would improve monitoring problem areas if they remain unobtrusive - through small form factors and simplified interrogation hardware.

Mass loss coupons operate under the principal that corrosion leads to mass loss. In a mass loss coupon, the mass loss is determined by removing the coupon from the structure and measuring the remaining material. This provides advantages such as visual interpretation of corrosion type and localization. Furthermore, many corrosion standards are based on the actual mass loss of a material, making this approach well-suited to standardization. This paper presents a new monitoring technique based on inductively coupled mass-loss coupons that combine many of the performance advantages of mass loss coupons with the integration advantages of electrical resistance probes.

In the corrosion monitoring approach, a “coupon” is fabricated with a sacrificial surface. The mass loss of these nanostructured coupons is measured using inductance rather than electrical resistance. Inductance represents a volume property of the coupon as opposed to the surface property of resistance. This readout approach allows a direct mass-loss measurement based on the change in the inductance of the coupon when placed in an alternating magnetic field.

The sensors will be coupled with low power electronics (passive sensor tag) and placed in multiple enclosed locations on aviation and missile platforms as shown in Fig. 1. The soldier, or maintenance expert will routinely utilize a sensor tag reader to wireless inspect for corrosion damage on the enclosed compartments of the platform.

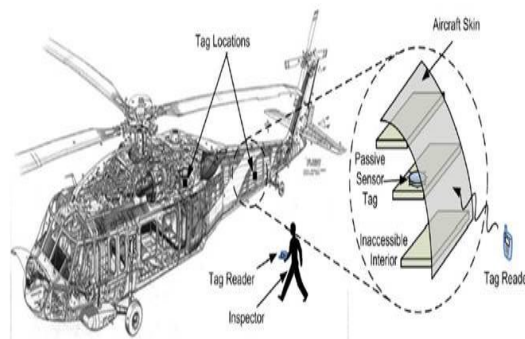


**Figure 1.** Conceptual application of corrosion sensors.

## 2. ARMY'S CURRENT METHOD FOR DETERMINING CORROSION

Currently, the military uses visual inspection during routine maintenance checks or pre-flight checks to diagnose corrosion damage. Visual inspection is costly, unreliable, destructive, and potentially inefficient. The routine inspections increase sustainment costs, and commonly, structures are discarded or destroyed for corrosion damage. Another detection method is radiography. Radiography is an imaging technique that uses electromagnetic radiation other than visible light, especially X-rays, to view the internal structure of a non-uniformly composed and opaque object. With this method, X-ray technology is used to inspect the inside of the potentially corroded metal surface. Ultrasonic testing, which is a type of nondestructive testing commonly used to find flaws in materials and to measure the thickness of objects, emits high frequency acoustic waves to determine the structural image, as shown in Fig. 2. Measurements of the Eddy Current of the material are also utilized in corrosion monitoring. The Eddy current is a localized electric current induced in a conductor by a varying magnetic field. It is caused when a conductor is exposed to a changing magnetic field due to relative motion of the field source and conductor; or due to variations of the field with time. Lastly, thermography, which is the use of thermograms to study heat distribution in structures or regions is used because corroding metals have a different temperature than non-corroding metals.



**Figure 2.** Current methods to detect corrosion damage.

## 3. SENSOR FABRICATION

The fabrication process for the nanomaterial coupon is based on automated sequential electrodeposition of ferromagnetic perm-alloy and sacrificial material, Figure 3a, followed by selective removal of the sacrificial layers so as to insulate each perm-alloy layer, Figure 3b. Copper was selected for the sacrificial material due to copper's exhibition of low surface roughness, high adhesion to the magnetic material, and copper has the ability to be selectively etched away without degrading or etching the magnetic material.

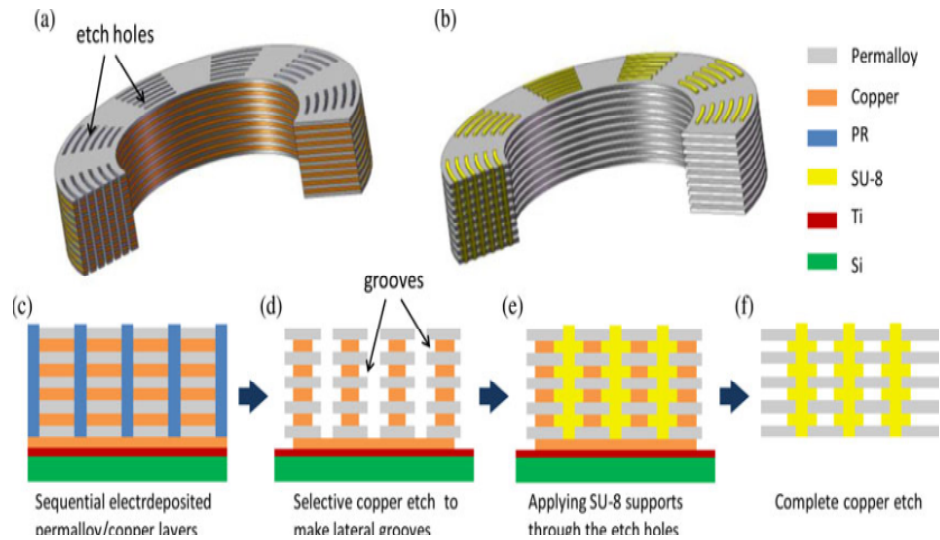


**Figure 3.** Fabrication process for the nano-laminated perm-alloy core: (a) Schematic of electrodeposited multilayers (eddy currents are dominant); (b) Schematic of the laminated metal/insulator structure (eddy currents are suppressed); (c) thru (f) Detailed sequence for the fabrication of the nano-laminated perm-alloy core.

The fabrication begins with forming a thick photoresist mold on top of a sputtered metallic seed layer. This mold is then filled with alternating layers of ferromagnetic Perm-alloy and copper using a robotic multilayer electrodeposition system, Figure 3c. The total thickness of the sequential electro deposition is linked to the thickness of the mold, which typically can vary from tens of micrometers to the millimeter-scale depending on the targeted thickness of the core. A Watts-type bath was employed for the electrodeposition of Perm-alloy<sup>1</sup>, and a commercial copper bath containing brighteners and levelers was utilized for copper electrodeposition.

After the photoresist mold is removed by acetone, a short selective copper wet etch is performed to create lateral “grooves” around the sidewall of the structure (see Figure 3d, above). The copper wet etch provides improved selectivity between a magnetic layer and copper. SU-8 epoxy<sup>2</sup> is then applied through the “etch holes” depicted in Figure 3e, which refer to the areas that were covered by the plating mold during the electrodeposition. A subsequent UV exposure and post-exposure bake allows for a portion of “etch holes” filled with cross-linked SU-8 to be left.

Next, the sacrificial copper layers are completely removed in the etchant through the periphery of the structure and the “etch holes” unoccupied by SU-8 so that individual laminations can be created, as shown in Figure 3f (above). Note that the nonconductive SU-8 in the “grooves” and etch holes allows the Perm-alloy layers to maintain their mechanical integrity after the copper removal, in comparison to the previous work where an additional electrodeposition of conductive structures was employed for the same purpose<sup>3</sup>. Through this approach, the complete electrical insulation between perm-alloy layers is feasible.

The nano-laminated cores are fabricated at the wafer level, as shown in Figure 4, with full batches of devices being fabricated simultaneously. The cores are released from the wafer after fabrication is complete.

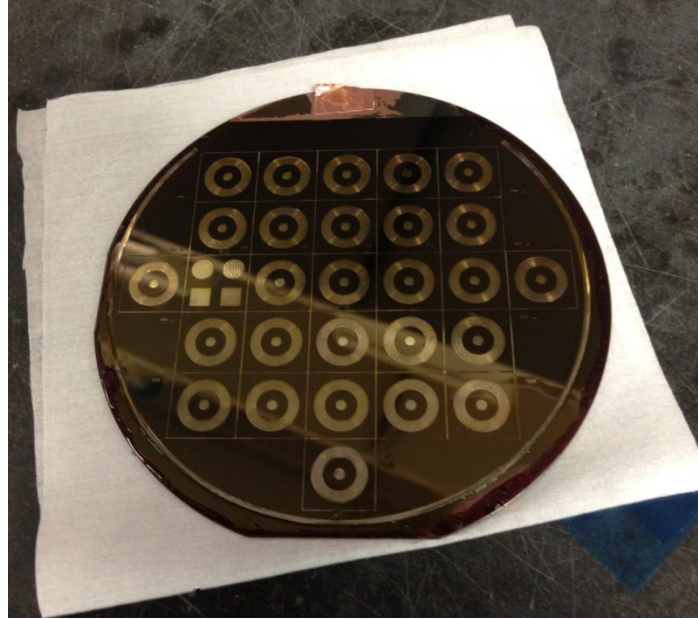


**Figure 4.** A full wafer of nano-laminated cores

These cores are then formed into electrical inductors by packaging them in laser-micro-machined polymeric bobbins and winding them with low-loss Litz wire. For the fabrication of a bobbin, the polymeric sheet is first laser-scribed to form a toroidal trench at the center where the magnetic core can be securely placed. The trench is slightly deeper than the core thickness and wider than the core outer diameter so that the released core structure does not collapse by subsequent manual coil winding. Then, a number of notches are cut along the periphery of the trench to provide space for tight and reproducible winding without overlap. Figure 5 shows fabricated inductors with laminated perm-alloy cores packaged in polymer bobbins, wound by Litz wire having either 36 or 48 turns.

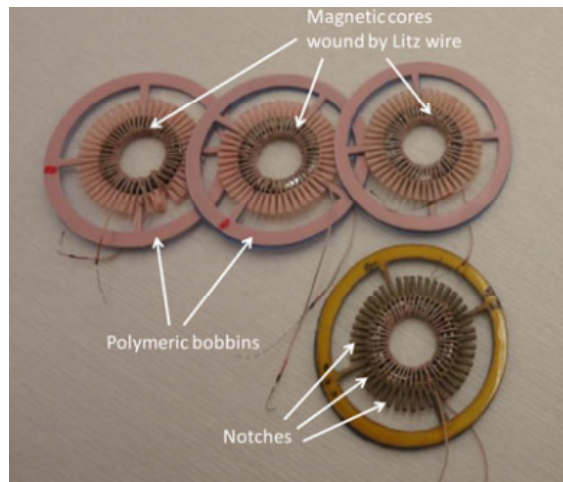


**Figure 5.** Fabricated inductors via packaging the magnetic cores in laser machined polymeric bobbins winding with Litz wire.

By scanning the inductor frequency response using a vector network analyzer, the inductance, capacitance, and resonance of the device can be characterized. The inductance of the inductor is dependent on the fabrication parameters as shown in Figure 6. These inductors also exhibit an inductance that changes with frequency, as well as a self-resonance at a particular frequency. The self-resonance, in particular, is a useful quantity that allows the inductor to be used as a

sensor, as this self-resonance will shift as the device's inductance changes.

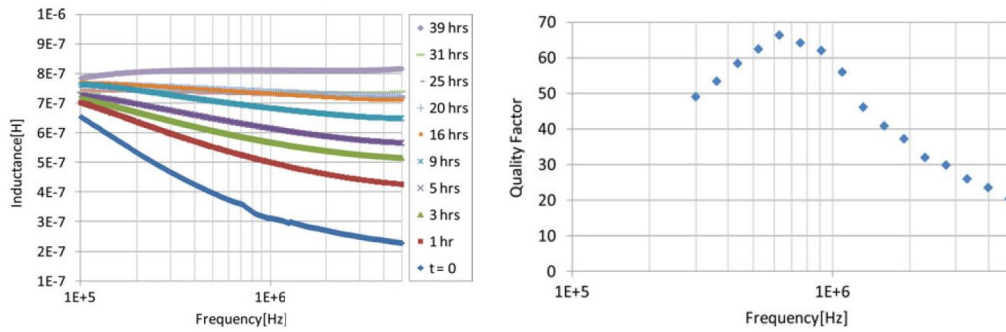


**Figure 6.** (a) Inductance change of the packaged inductor with respect to the etch time of the sacrificial layers. Individual low-frequency inductances are subject to compensation errors, but the frequency dependence of the inductance clearly shows the beneficial effect of interlamination conductor removal. (b) Inductor quality factor reaching as high as 60 at 1 MHz.

#### 4. EXPERIMENTAL SETUP

In order to determine the appropriate material to be used for the sacrificial sensing source, four types of metals and four corrosion sensors were aged at an accelerated pace. The metals consisted of Low Carbon Steel (LCS), Cold Rolled Steel (CRS), Galvanized Zinc (GZ), and Copper Plated Zinc (CPZ). Fig. 7 (below) shows all of the previously listed metals, respectively.



**Figure 7.** Sensor and material samples.

The corrosion sensor sensing element is a nanofabricated Nickel-Cobalt-Iron material, surrounded by copper wire, as shown in Fig. 8 (below).

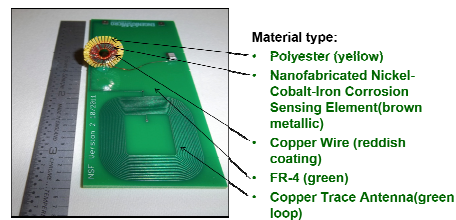


**Figure 8.** Photo of prototype corrosion Sensor apparatus & material composition



Prior to placing the sensors and material samples in the environmental chamber, the mass of each sample was measured. Measurable results are shown in Table 1. It is common knowledge that corrosion leads to mass loss. Expectations are for the mass of the samples to be measured at the conclusion of the accelerated aging experiment in order to determine total mass loss.

**Table 1.** Mass measurements of sensors and material samples

	Reference (1)	2	3	4	5
Sensor	N/A	N/A	N/A	N/A	N/A
Low Carbon Steel	N/A	N/A	N/A	N/A	N/A
Cold Roll Steel	35.3g	38.6g	36.7g	39.1g	37.7g
Galvanized Zinc	4.9g	4.9g	4.9g	4.9g	4.9g
Copper Plated Zinc	2.5g	2.5g	2.5g	2.5g	2.5g

The sensors and four types of metals were placed in an environmental chamber for the accelerated aging tests. The chamber was manually set at 122°F and 95.5% Relative Humidity, as shown below in Fig. 8 (below). The sensors and material samples were strategically placed for optimal environmental exposure. The sensors were additionally placed in the chamber in a manner that would make it convenient to take sensor read-outs. As also shown in Fig. 9 (below), two of the sensors are adjacent to the chamber surface, while two are suspended in the air. This arrangement allows for additional air flow and other environmental variances to affect the sensors. In order to allow for experimental comparisons, one sensor and a set of test samples (of each material) were not exposed to the chamber’s environmental conditions; thus, these reference specimens can be used to measure the changes in mass and inductance.



**Figure 9.** Experimental Setup

In order to measure the changes in the sensors without disturbing the aging experiment, test leads (positive and negative terminals) were draped outside the chamber. Data was collected every 30 minutes and/or hourly, with an inductance meter. The metals samples were measured for mass loss and examined with a scanning electron microscope (SEM) and numerous images were produced after several focused beam of electrons scans were conducted. As expected,

the SEM results clearly showed the magnitude of aging on both the sensor and associated metal specimens. The results clearly demonstrate the equivalence of corrosion that would be related to each specimen's lifecycle. Figure 10 (below) shows the salt/fog chamber with specimens associated with samples#2 underwent 200 hours of salt/fog exposure.

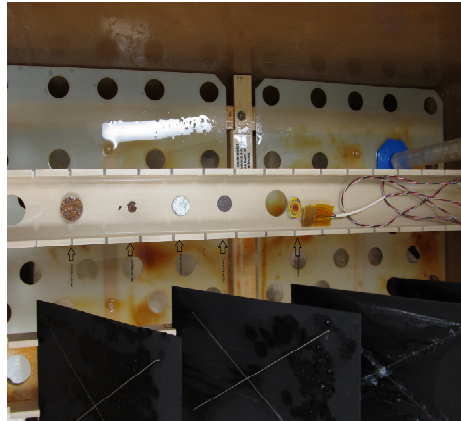


**Figure 10.** Photo of sensor and test samples in the salt fog chamber.

## 5. LABORATORY RESULTS

The sensors and samples, after being exposed to environmental conditions that equated to accelerated aging, visually showed corrosion after 306 hours in the environmental chamber. As expected, the corrosion increased significantly after additional exposures up to 2494 hours in the chamber. Results are shown in Fig. 11 (below). Specimens associated with samples#4 underwent 306 hours of 122 degrees F (at 95 percent relative humidity). In a similar manner (with more prolonged exposure), specimens associated with samples#5 underwent approximately 1505 hours of 122 degrees F (at 95 percent relative humidity). Samples#2 and samples#3 more aggressively experienced approximately 2494 hours of 122 degrees F (at 95 percent relative humidity). The low carbon steel specimen associated with samples#3 was misplaced. Additionally, specimens associated with samples#2 underwent 200 hours of salt/fog exposure; however, the low carbon steel specimen, exposed in the salt/fog chamber, virtually disintegrated.





**Figure 11.** Photo of sensor at room temp and ambient relative humidity (rh), along with metal samples (after 306 to 2494 hours at 122 degrees F and 95.5 percent rh.)

The data collected demonstrated the pattern of metal degradation and showed that repeatable sensor inductance measurements will allow for long-term environmental monitoring. As part of the future research, additional studies will be conducted to gather enhanced understanding of the influences associated with oxide growth and metal degradation within the sensor and its corresponding response.

The graphs (below in figure 12) show the data points and behavior of the sensors' response (inductance values) after up to 306 hours and/or more in the environmental chamber. As expected, the inductance values for each sensor decreased after exposures up to 2494 hours in the chamber. Results indicate that the commutative corrosion for each specimen can be equated to the accompany sensor's inductance output. As pervious outlined in the experiment, stated, the graph shows the decreased pattern of inductance output for the sensors associated with the specimens consequent to samples#4 (306 hours of 122 degrees F at 95 percent relative humidity); specimens associated with samples#5 (1505 hours of 122 degrees F at 95 percent relative humidity); and both samples#2 and #3 experiencing approximately 2494 hours of 122 degrees F at 95 percent relative humidity. Although the low carbon steel specimen associated with samples#3 was misplaced, the pattern of decreased inductance still applies. In a corresponding manner, the pattern of decreased inductance applies to the low carbon steel specimen consequent to samples#2 which underwent 200 hours of salt/fog exposure. As previously stated, the low carbon steel specimen (exposed in the salt/fog chamber) virtually disintegrated.

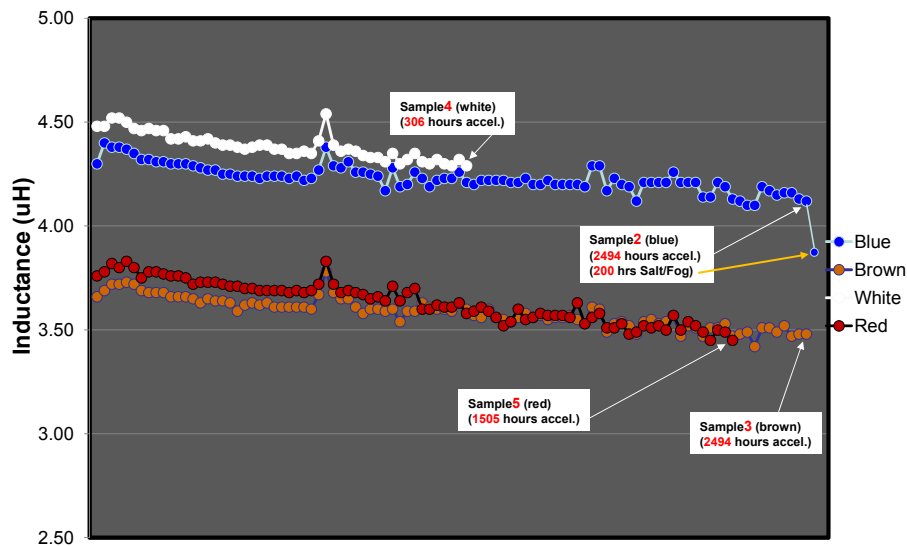


**Figure 12.** Inductance Sensor Measurements after environmental exposure

## 6. CONCLUSION

The ability to remotely read the inductance values of sensor coupons provides opportunities for sensors to be embedded in concealed compartments for applications associated with monitoring structural degradation. It allows the sensors to be read electronically using a low power system. The change in the inductance of the sensor demonstrated the unit's acceptable sensitivity and showed how it equates significantly to the metal structures' corrosion levels. Additionally, the self-resonant frequency of the devices could be used as an enhanced indication of corrosion levels. Measuring self-resonance can be simpler to perform using low-power electronics; thus, making nano-based sensor very attractive for the assessment of weaponry structural degradation.

## 7. FUTURE EFFORTS

The need for and use of embedded nano-based sensors can be a high priority for military aircraft. The need becomes greater and there will be a greater low-cost maintenance priority as the U.S. defense budget continues to decrease. The overall scenario makes it very important to continue affording high-cost maintenance associated with weaponry structural degradation. Relative to the nano-based sensor, future efforts will include additional testing and sensor implementation with corresponding stand-off electronic readers.

## REFERENCES

- [1] Park, J. Y., “Packaging-compatible micromachined magnetic devices: Integrated passive components and modules,” Ph.D. dissertation, Dept. Electr. Comput. Eng., Georgia Institute of Technology, Atlanta, GA, USA (Dec. 1997)
- [2] [http://www.microchem.com/Prod-SU8\\_KMPR.htm](http://www.microchem.com/Prod-SU8_KMPR.htm)
- [3] Han, Y., Cheung, G., Li, A., Sullivan, C. R., and Perreault, D. J., “Evaluation of magnetic materials for very high frequency power applications,” in Proc. IEEE Power Electron. Spec. Conf., pp. 4270–4276 (Jun. 2008)